Photoluminescence in integer quantum Hall systems

Kenichi Asano
Department of Physics, University of Tokyo, 7-3-1 Hongo, Bunkyou-ku, Tokyo 113-0033, Japan

Tsuneya Ando
Institute for Solid State Physics, University of Tokyo, 5-1-5 Kashiwanoha, Kashiwa, Chiba 277-8581, Japan
(Received 6 August 2001; published 8 March 2002)

Photoluminescence spectra in two-dimensional systems in the quantum Hall regime $\nu \geqslant 2$ are studied using a numerical diagonalization method, where ν is the filling factor. The first moment of the spectra is understood in terms of the ν-dependent screening effect. The spectra of left-circularly polarized light usually exhibit a double-peak structure when $2<\nu \leqslant 4$, in qualitative agreement with recent experiments. Those of right-circularly polarized light show only a single peak when $2 \leqslant \nu \leqslant 3$ and a double-peak structure when $3 \leqslant \nu \leqslant 4$. The origin of this double-peak structure is strong hybridization between optically allowed and forbidden final states through inter-Landau-level scattering between electrons with opposite spins.

DOI: 10.1103/PhysRevB.65.115330 PACS number(s): 73.43.−f, 78.55.−m

I. INTRODUCTION

For the past two decades, photoluminescence (PL) has been intensively studied both experimentally[1–25] and theoretically[26–59] in two-dimensional (2D) systems in the quantum Hall (QH) regime. In this paper, we investigate electron-electron (*e-e*) and electron-hole (*e-h*) interaction effects on PL in QH systems characterized by the filling factor $2 \leqslant \nu \leqslant 4$. Exact spectra in finite-size systems are calculated using a numerical diagonalization method including their first moment.

Experiments are performed in various type of systems: for example, quantum wells (QW's),[1–11,22–25] normal single heterojunctions,[12–18] and single heterojunctions with an acceptor monolayer.[19–21] In this paper, we mainly discuss PL in QW's. When a QW is sufficiently narrow, electrons and a photoexcited valence hole can be regarded as being confined in a same 2D plane as shown in Fig. 1(a). In this case, the potential of *e-e* and *e-h* interactions satisfies the relation $v^{ee}(r)=-v^{eh}(r)$. When the QW is skewed as is shown in Fig. 1(b) due to one-side doping or an external electric field, electrons and a photoexcited valence hole are confined in layers separated by a distance d and therefore $v^{ee}(r)>-v^{eh}(r)$. This *e-h* layer distance d can be controlled by an external electric field applied normal to the interface with a gate electrode structure.

When a conduction electron with spin $s_z=+\hbar/2$ and a valence heavy hole with angular momentum $j_z=-3\hbar/2$ are recombined, left-circularly polarized (LCP) light is emitted. On the other hand, a recombination of an electron with spin $s_z=-\hbar/2$ and a hole with angular momentum $j_z=+3\hbar/2$ induces right-circularly polarized (RCP) light.

Photoluminescence at $\nu>2$ is intriguing from the point of view of symmetry breaking. When electrons and a photoexcited valence hole are confined in the same 2D plane and all of them belong to the lowest Landau level, the system possesses a ''hidden symmetry'' [26–29] expressed by a commutation relation between the Hamiltonian projected onto the lowest Landau level $\bar{\mathcal{H}}$ and the recombination operator $\mathcal{L}_\alpha$:

$$[\bar{\mathcal{H}},\mathcal{L}_\alpha]=-(E_\alpha^0-E_0)\mathcal{L}_\alpha, \tag{1.1}$$

where subscript $\alpha=-$ and $+$ denote LCP and RCP light, respectively, E_α^0 is the PL energy in the absence of many-body effects, and E_0 is the binding energy of a magnetoexciton consisting of an electron and a valence heavy hole in the lowest Landau level. Due to this commutation relation, PL spectra are always proportional to $\delta(E-E_\alpha^0+E_0)$ independent of the electron filling factor ν and the PL energy gives only trivial information on many-body effects.

This symmetry is destroyed and PL spectra are directly modified in their energies and structures when electrons and a valence hole are confined in layers separated by a distance $d>0$ or an excited Landau level is occupied by some electrons. The symmetry breaking at $\nu>2$ is caused by inter-Landau-level *e-e* scattering, where an electron in an excited Landau level is relaxed to the lowest one to fill the unoccupied state left after the recombination and another electron is excited to the excited Landau level.

Figure 2 shows some examples of the inter-Landau-level *e-e* scattering, which occurs after LCP photoemission at $\nu>2$. It can be classified according to the spin of scattered electrons. When relaxed and excited electrons have the same spin as shown in Figs. 2(b) and 2(c), we call the process

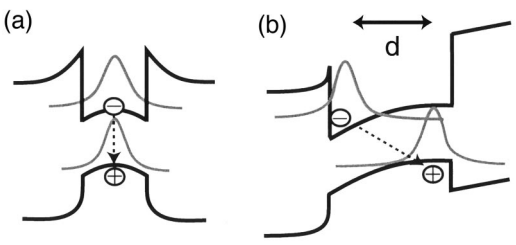

FIG. 1. Schematic figures of the quantum well. (a) A narrow and symmetric quantum well. (b) A wide and asymmetric quantum well, where d is the distance between the electron and hole layers.

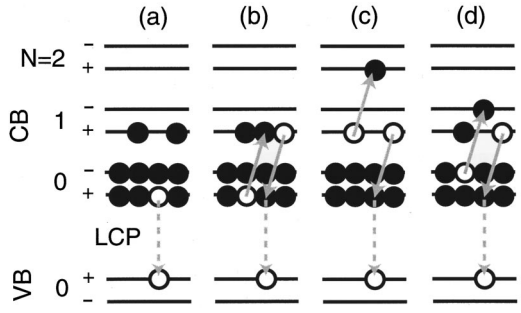

FIG. 2. Some examples of inter-Landau-level *e-e* scattering which occurs after LCP photoemission. (a) Just after the LCP photoemission. (b),(c) Inter-Landau-level scattering in which the relaxed and excited electron have the same spin (same-spin scattering). (d) Scattering between electrons with different spins (opposite-spin scattering).

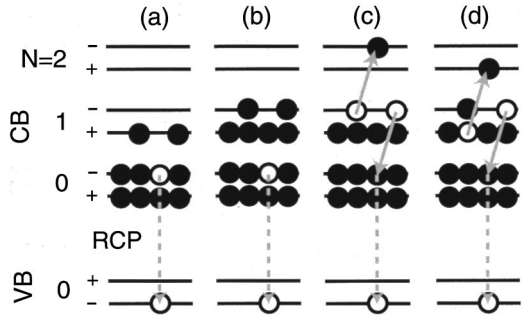

FIG. 3. Some examples of inter-Landau-level *e-e* scattering which occurs after RCP photoemission. (a) Just after the RCP photoemission when $2 \leqslant \nu \leqslant 3$. Inter-Landau-level *e-e* scattering is forbidden because there is no down-spin electron in the first excited Landau level. (b) Just after RCP photoemission when $\nu > 3$. (c) Same-spin scattering (d) Opposite-spin scattering.

same-spin scattering. On the other hand, it is named opposite-spin scattering when they have opposite spins as shown in Fig. 2(d).

When the Zeeman splitting is large enough to polarize the electron spin maximally, inter-Landau-level *e-e* scattering is forbidden for RCP photoemission in the case $2 < \nu \leqslant 3$. This is because there are no down-spin electrons in excited Landau levels as shown in Fig. 3(a). In this case, the hidden symmetry still remains and spectra become a single δ function located at $E = E_+^0 - E_0$, when electrons and a valence hole are confined in the same layer ($d = 0$). At $\nu > 3$ inter-Landau-level *e-e* scattering becomes allowed for RCP photoemission as is schematically shown in Figs. 3(b), 3(c), and 3(d).

The screening effect is another keyword to understand PL in the QH regime. This has been the main interest of the early perturbation theories,[30–34] in which the many-body correction to the PL energy is approximately calculated as the sum of the electron self-energy Σ^e and the hole self-energy Σ^h without Zeeman splittings. The hole self-energy Σ^h describes the energy reduction by attraction of electrons around the hole. The electron self-energy Σ^e consists of two contributions: the Coulomb hole term $\Sigma^e_{\rm CH}$ and screened exchange $\Sigma^e_{\rm XS}$. The hole self-energy Σ^h and the Coulomb hole term $\Sigma^e_{\rm CH}$ show upward cusps around at even integer filling factors $\nu = 2n$ (n: integer) and a downward convex curve when $2n < \nu < 2(n+1)$. On the contrary, $\Sigma^e_{\rm XS}$ exhibits downward cusps around at $\nu = 2n$ and an upward convex curve when $2n < \nu < 2(n+1)$. Because the magneto-oscillations of $\Sigma^e_{\rm CH}$ and $\Sigma^e_{\rm XS}$ are almost canceled out, Σ^e shows only weak downward cusps at even integer filling factors. Thus, when the *e-h* layer distance d is much smaller than the magnetic length l, the hole self-energy dominates the filling factor dependence of PL energy. However, it is determined by the oscillation of electron self-energy when $d \gg l$, because the hole self-energy Σ^h is strongly suppressed.

These diagrammatic theories in which the broadening of Landau levels is introduced by disorder could qualitatively reproduce magneto-oscillation of the PL energy observed in early experiments.[1] Recently, PL spectra were calculated in spinless systems without disorder for $1 \leqslant \nu \leqslant 3$ by a numerical diagonalization method,[52,53] which has been used in previous numerical studies on the fractional QH regime $\nu \leqslant 1$.[37–51] The results show PL energy oscillations similar to those obtained in perturbation calculations when the *e-h* layer distance is small ($d \ll l$). In fact, photoluminescence energy exhibits a downward convex curve when $1 < \nu < 2$ and $2 < \nu < 3$ and an upward cusp at $\nu = 2$. When it is large ($d \gg l$), the magnitude of the oscillation is suppressed and PL energy is shifted almost linearly as a function of the filling factor.

Unfortunately, such calculations are still unsatisfactory because the electron spin sometimes drastically affects PL spectra in line shapes.[54,55] In fact, it is shown that spectra of the LCP light around at $\nu = 3$ show peak splitting caused by opposite-spin scattering, which is absent in spinless systems. Such a double-peak structure in LCP spectra has been experimentally observed not only around at $\nu = 3$, but in the wide range of the filling factor $\nu > 2$.[22–25] In this paper, it will be shown that the LCP spectra exhibit a double-peak structure in the whole range of $2 < \nu \leqslant 4$, even when there is only a single electron in the first excited Landau level ($\nu = 2^+$).

II. MODEL AND HAMILTONIAN

In our model of the QW system, the electron and hole layers have square geometries ($0 \leqslant x \leqslant a$, $0 \leqslant y \leqslant a$) and their thickness is ignored. A uniform magnetic field B is applied normal to the interface and a periodic boundary condition is used in both x and y directions.[60–63] The area of the system is not arbitrary, but given by

$$A = a^2 = 2\pi l^2 N_\phi, \tag{2.1}$$

where the magnetic length is defined by $l = \sqrt{\hbar/eB}$ with electron charge $-e$ and the integer N_ϕ denotes the number of flux quanta passing through the system.

Using the Landau gauge $\mathbf{A}(\mathbf{r}) = (0, Bx)$, the orbital wave functions of a single electron and hole are defined by

$$\psi^e_{NX}(\mathbf{r}) = \phi_{NX}(\mathbf{r}),$$

$$\psi^h_{NX}(\mathbf{r}) = \phi^*_{NX}(\mathbf{r}), \tag{2.2}$$

with

$$\phi_{NX}(\mathbf{r})=\left(\frac{1}{2^N N!\sqrt{\pi}al}\right)^{1/2}\sum_{m=-\infty}^{+\infty}H_N\left(\frac{x-X-ma}{l}\right)\times\exp\left[-i\frac{X+ma}{l^2}y-\frac{(x-X-ma)^2}{2l^2}\right], \quad (2.3)$$

where H_N is the Hermite polynomial and X is the x coordinate of the guiding center, which takes the discrete N_ϕ values

$$X=\frac{2\pi l^2}{a}j=\frac{a}{N_\phi}j \quad (j=0,1,...,\ N_\phi-1). \quad (2.4)$$

The creation and annihilation operators of a conduction electron characterized by the orbital wave function ψ^e_{NX} and the spin $\hbar\sigma/2$ are written as $e^\dagger_{\xi\sigma}$ and $e_{\xi\sigma}$ with $\xi=(NX)$, respectively. Similarly, $h^\dagger_{\xi\sigma}$ and $h_{\xi\sigma}$ are defined as the creation and annihilation operators of a valence hole characterized by the orbital wave function ψ^h_{NX} and spin $3\hbar\sigma/2$, respectively. For charge neutrality, a background positive charge $(N_e-N_h)e$ is spread uniformly on the electron layer, where N_e and N_h are the number of electrons and holes, respectively. Note that N_e-N_h is conserved in the photoemission process.

Because the hole-hole interaction is negligible in the limit of vanishing hole density, the Hamiltonian is written as

$$\mathcal{H}=\sum_{\xi\sigma}\epsilon^e_{N\sigma}e^\dagger_{\xi\sigma}e_{\xi\sigma}+\sum_{\xi\sigma}\epsilon^h_{N\sigma}h^\dagger_{\xi\sigma}h_{\xi\sigma}+\frac{1}{2}\sum_{\{\xi_i\}}\sum_{\sigma\sigma'}V^{ee}_{\xi_1\xi_2\xi_3\xi_4}e^\dagger_{\xi_1\sigma}e^\dagger_{\xi_2\sigma'}e_{\xi_3\sigma'}e_{\xi_4\sigma}+\sum_{\{\xi_i\}}\sum_{\sigma\sigma'}V^{eh}_{\xi_1\xi_2\xi_3\xi_4}e^\dagger_{\xi_1\sigma}h^\dagger_{\xi_3\sigma'}h_{\xi_2\sigma'}e_{\xi_4\sigma}+\frac{e^2d}{2\epsilon A}N_h^2, \quad (2.5)$$

with

$$\epsilon^e_{N\sigma}=\epsilon^e_{\rm bot}+\hbar\omega_e\left(N+\frac{1}{2}\right)+\frac{\sigma}{2}g_e\mu_B B,$$

$$\epsilon^h_{N\sigma}=\epsilon^h_{\rm bot}+\hbar\omega_h\left(N+\frac{1}{2}\right)+\frac{\sigma}{2}g_h\mu_B B,$$

$$V^{ij}_{\xi_1\xi_2\xi_3\xi_4}=\frac{1}{A}\sum_{\mathbf{q}\neq0}v^{ij}_q A^{N_1N_4}_{-\mathbf{q}}A^{N_2N_3}_{\mathbf{q}}B^{X_1X_4}_{-\mathbf{q}}B^{X_2X_3}_{\mathbf{q}}, \quad (2.6)$$

where indices $i,j=e,h$ denote electron and hole, respectively, $\epsilon^i_{\rm bot}$ is the energy bottoms of the ground subband, ω_i is the cyclotron energy, g_i indicates the g factor, $\mathbf{q}=(2\pi m/a,2\pi n/b)$ $(m,n$: integer) denotes the reciprocal vector, Fourier components of Coulomb interaction are given by

$$v^{ee}_q=\frac{e^2}{2\epsilon q},$$

$$v^{eh}_q=-\frac{e^2}{2\epsilon q}\exp(-qd), \quad (2.7)$$

the Landau-orbit form factor is defined by

$$A^{NN'}_{\mathbf{q}}=\begin{cases}\sqrt{\dfrac{N'!}{N!}}\left[\dfrac{(iq_x+q_y)l}{\sqrt{2}}\right]^{N-N'}L^{N-N'}_{N'}\left(\dfrac{q^2l^2}{2}\right)\exp\left(-\dfrac{q^2l^2}{4}\right) & (N\geqslant N'),\\ \sqrt{\dfrac{N!}{N'!}}\left[\dfrac{(iq_x-q_y)l}{\sqrt{2}}\right]^{N'-N}L^{N'-N}_{N}\left(\dfrac{q^2l^2}{2}\right)\exp\left(-\dfrac{q^2l^2}{4}\right) & (N<N'),\end{cases} \quad (2.8)$$

with an associated Laguerre polynomial $L^m_n(x)$, and the guiding-center form factor is defined by

$$B^{XX'}_{\mathbf{q}}=\delta'_{q_yl^2,X'-X}\exp\left[\frac{i}{2}q_x(X+X')\right], \quad (2.9)$$

with the modified δ function

$$\delta_{XX'}=\begin{cases}1 & (X-X'=na,n:\ \text{integer}),\\ 0 & (\text{otherwise}).\end{cases} \quad (2.10)$$

The last term $(e^2d/2\epsilon A)N_h^2$ on the right-hand side of Eq. (2.5) denotes the charging energy captured in the electron and hole layers and negligible in the thermodynamic limit $(A\to\infty)$.

Now, let us introduce the characteristic Coulomb energy

$$E_C=\frac{e^2}{4\pi\epsilon l}, \quad (2.11)$$

with the dielectric constant ϵ, and consider the high-magnetic-field limit $E_C\ll\hbar\omega_e,\hbar\omega_h$. We also assume k_BT

$\ll \hbar\omega_e, \hbar\omega_h$, where k_B is the Boltzmann constant and T denotes temperature. In these limits, the photoexcited valence hole belongs to the lowest Landau level. However, it has to be noted that the assumption $E_C \ll \hbar\omega_h$ is not easily realized in usual experimental systems due to the heavy mass of the valence hole. It is possible that some substructures appear in spectra when the valence hole occupies excited Landau levels.

The initial states are configurations of N_+ up-spin electrons, N_- down-spin electrons, and a single photoexcited valence hole. The electron filling factor is given by $\nu = \nu_+ + \nu_-$, where $\nu_+ = N_+/N_\phi$ and $\nu_- = N_-/N_\phi$ are the filling factor of the up-spin and down-spin electrons, respectively. In the following, we mainly consider the large Zeeman limit in which the electron spin is maximally polarized. This implies that ν_+ and ν_- are given by

$$(\nu_+, \nu_-) = \begin{cases} (\nu-1, 1) & (2 \leqslant \nu \leqslant 3), \\ (2, \nu-2) & (3 \leqslant \nu \leqslant 4), \end{cases} \tag{2.12}$$

in the initial states. Experimentally, such a condition is realized in narrow gap semiconductors.[8,9] The spin-flipping effects caused by small Zeeman splittings will be discussed in the last part of this paper.

The *e-h* recombination operators of LCP ($\alpha = -$) and RCP ($\alpha = +$) photoemission are defined by

$$\mathcal{L}_- = \sum_X e_{0X+} h_{0X-},$$

$$\mathcal{L}_+ = \sum_X e_{0X-} h_{0X+}, \tag{2.13}$$

respectively. Diagnonalizing the Hamiltonian numerically, we obtain all initial and final states of the finite-size system. Then, LCP and RCP photoemission spectra are calculated as

$$P_\alpha(E) = \sum_{i,f} \frac{1}{Z} \exp\left(-\frac{E_i}{k_B T}\right) |\langle f|\mathcal{L}_\alpha|i\rangle|^2 \delta(E - E_i + E_f), \tag{2.14}$$

where i and f are the indices of initial and final states, respectively, E_i and E_f are their energies, and Z is the partition function. Because the lowest Landau level is fully occupied in the initial states, we obtain the intensity sum rule

$$I_\alpha = \int P_\alpha(E) dE = \langle \mathcal{L}_\alpha^\dagger \mathcal{L}_\alpha \rangle_{\rm eq} = \frac{1}{2}\left(1 - \alpha \tanh \frac{|g_h|\mu_B B}{2 k_B T}\right), \tag{2.15}$$

where $\langle \cdots \rangle_{\rm eq}$ denotes the thermal average. This means that RCP spectra disappear in the low-temperature limit. However, some experiments indicate that the spin relaxation time is very slow and thermal equilibrium for the hole spin is not realized before *e-h* recombination, because RCP photoemission is observed even at low temperature. Therefore, we will not discuss the intensity of PL spectra any more and focus on the normalized spectra $\tilde{P}_\alpha(E) = P_\alpha(E)/I_\alpha$ in the following.

III. SCREENING EFFECTS ON THE PL ENERGY

In the high-magnetic-field limit, the first moment of the spectra is calculated as

$$E_\alpha^M = \int E \tilde{P}_\alpha(E) dE = -\frac{1}{I_\alpha} \langle \mathcal{L}_\alpha^\dagger [\mathcal{H}, \mathcal{L}_\alpha] \rangle_{\rm eq}. \tag{3.1}$$

Because it can be obtained without information of the final state $|f\rangle$, it is more easily calculated than the full PL spectra. In the regime $\nu \geqslant 2$, we obtain

$$E_\alpha^M = E_g - \langle g | \mathcal{L}_\alpha^\dagger \mathcal{H} \mathcal{L}_\alpha | g \rangle, \tag{3.2}$$

at absolute zero temperature, where $|g\rangle$ is the ground initial state when the angular momentum of the hole is fixed to $j_z = 3\hbar\alpha/2$ and E_g denotes its energy. The PL spectra are exactly given by $\tilde{P}_\alpha(E) = \delta(E - E_\alpha^M)$, if $\mathcal{L}_\alpha|g\rangle$ is an energy eigenstate.

Inter-Landau-level *e-e* scattering can contribute to the first moment of spectra when and only when it conserves both the number and spin of electrons in each Landau level. In the regime $2 \leqslant \nu \leqslant 4$, for example, E_α^M depends on same-spin scattering where an electron is relaxed from the first excited to the lowest Landau level and another electron is excited from lowest to first excited. However, it is unaffected by both opposite-spin and same-spin scattering where an electron is relaxed from the first excited to the lowest Landau level and another electron is excited from first excited to second excited.

Let us define the shifts of the first moment by

$$\Delta E_\alpha^M = E_\alpha^M - E_\alpha^0 + E_0, \tag{3.3}$$

where the PL energy in the absence of interaction is explicitly written as

$$E_\alpha^0 = \epsilon_{0-\alpha}^e + \epsilon_{0\alpha}^h + \frac{e^2 d}{2\epsilon A}, \tag{3.4}$$

and the binding energy of a magnetoexciton in the lowest Landau level with zero wave vector at $d = 0$ is defined by

$$E_0 = \frac{1}{A} \sum_{\mathbf{q} \neq \mathbf{0}} |A_{\mathbf{q}}^{00}|^2 v_q^{ee} \to \sqrt{\frac{\pi}{2}} E_C \quad (N_\phi \to \infty). \tag{3.5}$$

In the large Zeeman limit, we obtain

$$\Delta E_+^M(\nu+1) = \Delta E_-^M(\nu),$$

$$\Delta E_-^M(\nu+1) = \Delta E_+^M(\nu) - E_1, \tag{3.6}$$

with

$$E_1 = \frac{1}{A} \sum_{\mathbf{q} \neq \mathbf{0}} |A_{\mathbf{q}}^{10}|^2 v_q^{ee} \to \frac{1}{2}\sqrt{\frac{\pi}{2}} E_C \quad (N_\phi \to \infty). \tag{3.7}$$

Therefore, we have only to calculate the first moment of LCP spectra ΔE_-^M.

If the *e-h* correlation is ignored [Hartree-Fock (HF) approximation], ΔE_α^M can be estimated as

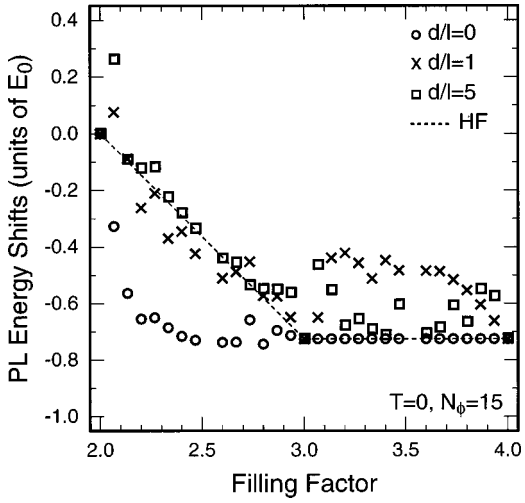

FIG. 4. Filling factor dependence of the first moment of LCP spectra calculated at $d/l=0$, 1, and 5 is shown with circles, crosses, and squares, respectively. Energy shifts are measured from $E_-^0 - E_0$ in units of E_0, where E_-^0 is the PL energy in the absence of many-body effects and E_0 denotes the binding energy of a magnetoexciton in the lowest Landau level. The dotted line shows the PL energy shift in the absence of correlation between electrons and a photoexcited valence hole (HF approximation).

$$\Delta E_-^M(\mathrm{HF}) = \begin{cases} -(\nu-2)E_1 & (2 \leqslant \nu \leqslant 3), \\ -E_1 & (3 \leqslant \nu \leqslant 4), \end{cases}$$

$$\Delta E_+^M(\mathrm{HF}) = \begin{cases} 0 & (2 \leqslant \nu \leqslant 3), \\ -(\nu-2)E_1 & (3 \leqslant \nu \leqslant 4). \end{cases} \tag{3.8}$$

At integer filling factors, where the Landau levels are completely occupied, these results become exact.

The shift ΔE_-^M calculated in a system with $N_\phi=15$ is shown in Fig. 4. Numerical results at the *e-h* layer distance $d/l=0$, 1, and 5 are exhibited with circles, crosses, and squares, respectively. The Hartree-Fock results are also shown by the dotted line.

When the electrons and the valence hole are confined in the same layer ($d=0$), ΔE_-^M is discontinuously shifted to the low-energy side at $\nu=2^+$, shows a downward convex curve for $2^+<\nu<3$, and becomes independent of the filling factor for $3 \leqslant \nu \leqslant 4$. In this case, the initial-state energy E_g is decreased by the accumulation of electrons in the first excited Landau level around the valence hole (screening effect). The averaged final-state energy $\langle g|\mathcal{L}_-^\dagger \mathcal{H} \mathcal{L}_-|g\rangle$ decreases also due to the attractive interaction between electrons in the first excited Landau level and the ''conduction hole'' left in the lowest up-spin Landau level after the LCP photoemission. It is expected that such screening effects are most enhanced when the first excited up-spin Landau level is nearly half-filled.

In the case $2 \leqslant \nu \leqslant 3$, the screening effect in the final-state energy is partially canceled by same-spin scattering in which an up-spin electron is relaxed from the first excited to lowest Landau level and another up-spin electron is excited from lowest to first excited. As a result, the screening effect in ΔE_-^M is dominated by that of the initial state and its ν dependence exhibits a downward convex curve. On the other hand, this kind of scattering is absent in $3 \leqslant \nu \leqslant 4$, because the first Landau level of the up-spin electron is completely occupied. As a result, ΔE_-^M becomes constant because the screening effect is exactly canceled out between the initial and final states.

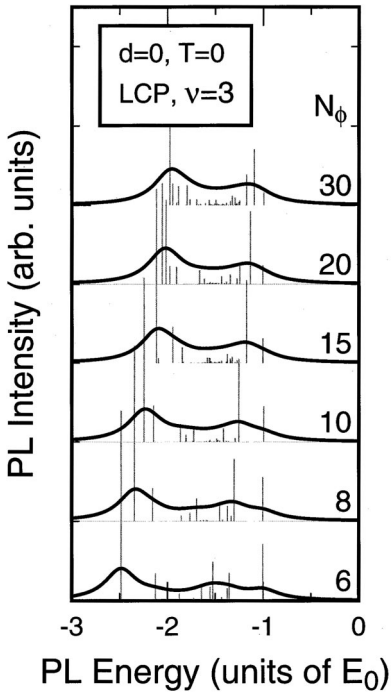

FIG. 5. LCP spectra at $T=0$ calculated numerically in systems with various sizes ($N_\phi=6$, 8, 10, 15, 20, and 30). The thin dotted lines show the histogram with width $\Delta/100$, and the solid lines exhibit the spectra broadened by a Lorentzian with half width $\Delta/5$.

At the intermediate *e-h* layer distance ($d/l=1$), the bowing effects in the region $2^+<\nu<3$ are suppressed and the moment shows an upward convex curve when $3<\nu<4$. As a result, ΔE_-^M exhibits a downward cusp at $\nu=3$. This is because the attractive interaction between electrons in the first Landau level and the valence hole is weakened by the *e-h* layer distance and the screening effect in the initial state is suppressed.

When the *e-h* layer distance is much larger than the magnetic length ($d/l=5$), ΔE_-^M exhibits no clear bowing effects and comes closer to the HF result though oscillating irregularly. This irregular oscillation is presumably because *e-e* repulsive interaction suppresses the accumulation of electrons around the hole and its effect changes sensitively as a function of ν due to finite-size effects.

At $\nu=2^+$ and 3^+, ΔE_-^M shows a large discontinuous blueshift and large discrepancy from the HF result. In these exceptional cases, the initial state $|g\rangle$ and the state after LCP photoemission $\mathcal{L}_-|g\rangle$ are those of a single exciton. Because the binding energy of an exciton is larger in final states than in the initial state, the first moment is blueshifted.

IV. PL SPECTRA IN FINITE-SIZE SYSTEMS

The full PL spectra numerically calculated in finite-size systems will be shown by both histograms with width

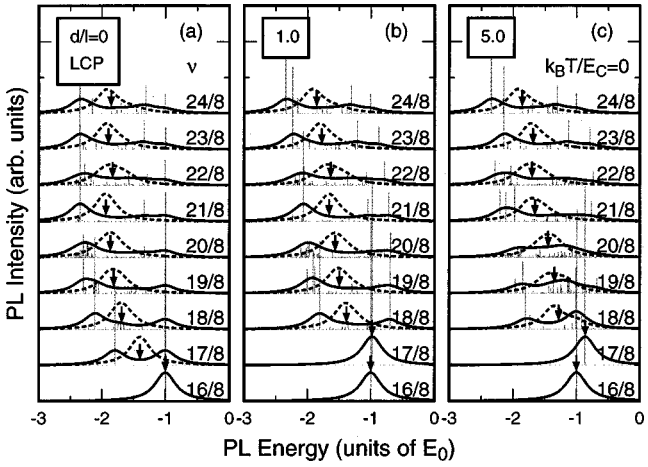

FIG. 6. LCP spectra at $T=0$ calculated at (a) $d/l=0$, (b) 1, and (c) 5 in the filling-factor range $2\leqslant\nu\leqslant 3$. The dashed lines show the spectra in a spinless fermion system at the corresponding filling factor $\nu_{\mathrm{sl}}=\nu-1$, which are equivalent to those calculated without opposite-spin scattering. The first moments of spectra are also indicated by arrows.

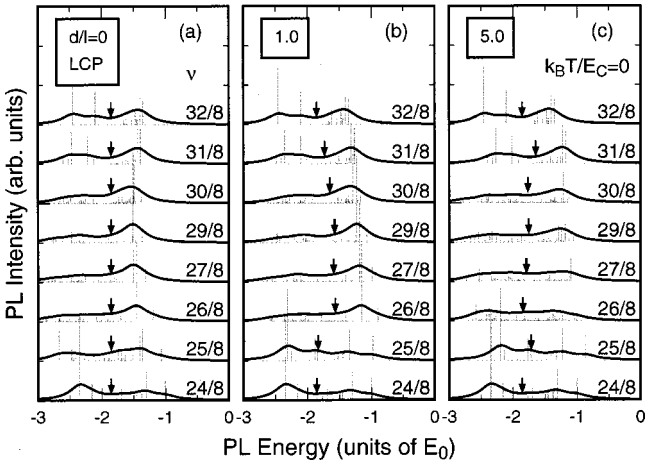

FIG. 7. LCP spectra at $T=0$ calculated at (a) $d/l=0$, (b) 1, and (c) 5 in the case $3\leqslant\nu\leqslant 4$.

$E_0/100$ (gray spikes) and convolutions with a Lorentzian with half width $E_0/5$ (solid lines). To investigate pure many-body effect, PL energies are measured from E_α^0 in units of magnetoexciton binding energy E_0 calculated in finite-size systems.

To check the system-size dependence of results, we calculate LCP spectra in the case $\nu=3$, $d=0$, and $T=0$ in various system sizes $N_\phi=6$, 8, 10, 15, 20, and 30, as shown in Fig. 5. As the system size is increased, δ-function peaks increase in their number and are shifted to the high-energy side. However, the broadened spectra always show a double-peak structure independent of the system size as long as $N_\phi\gtrsim 6$. In the following, PL spectra calculated in the system characterized by $N_\phi=8$ are discussed in more detail.

A. LCP spectra at zero temperature

The LCP spectra for $2\leqslant\nu\leqslant 3$ calculated at $d/l=0$, 1, and 5 are shown in Fig. 6. We also show broadened PL spectra calculated in spinless systems at the corresponding filling factor $\nu_{\mathrm{sl}}=\nu-1$ with dashed lines. They are equivalent to spectra calculated without opposite-spin scattering, because the Hamiltonian in the spinless fermion system is derived when the spin of the electrons and the valence hole are fixed to $+\hbar/2$, and $-3\hbar/2$ in Eq. (2.5), respectively. In general, the spectra consist of a huge number of δ functions. However, the spectra to which a sufficiently large broadening is introduced show two peaks with comparable intensities, when the electrons and hole have a spin degree of freedom. In contrast, they exhibit only a single peak in spinless systems. This fact clearly shows that the double-peak structure in LCP spectra is caused by opposite-spin scattering.

When the *e-h* layer distance is small ($d/l\ll 1$), the first moment of spectra shown by the arrows is shifted exhibiting an almost smooth downward convex curve as a function of ν. The energy shifts of the low-energy peak show an almost smooth downward convex curve, while those of the high-energy peak show only a small bowing effect. When the *e-h* layer distance is large ($d/l\gg 1$), the first moment of the spectra is almost linearly shifted and two peaks show no clear bowing effect in their energy shifts. In general, the magnitude of the peak splitting is enhanced with the increase of the filling factor ν and suppressed with the increase of the *e-h* layer distance d.

The PL spectra suddenly split into two peaks at $\nu=2^+$ when the *e-h* layer distance is small ($d/l\ll 1$). In this case, the initial ground state is characterized by a finite wave vector ($k\neq 0$) and the spectrum splits into two δ functions because the opposite-spin scattering gives rise to a mode repulsion of the final states. On the other hand, this splitting is absent and the spectrum is suddenly shifted to the higher-energy side at $\nu=2^+$, when the distance is large ($d/l\gg 1$). This is because the ground initial state is realized at $k=0$ and the opposite-spin scattering vanishes due to Kohn's theorem. A more detailed analysis of such behaviors will be given in the next section.

The LCP spectra for $3\leqslant\nu\leqslant 4$ calculated at $d/l=0$, 1, and 5 are shown in Fig. 7. Again, the spectra consist of a huge number of δ functions, but it seems that they have a double-peak structure again, if a sufficiently large broadening is introduced.

When electrons and the valence hole are confined in the same layer ($d=0$), the first moment has no filling-factor dependence when $2\leqslant\nu\leqslant 3$. However, it seems that the low- and high-energy peaks exhibit shifts of downward convex curves and their intensity is transferred from one to the other. The first moment shows an upward convex curve at $d/l\sim 1$ and an almost linear shifts at $d/l\gg 1$. The shifts of the low- and high-energy peaks are only weakly dependent on the *e-h* layer distance at $d/l\gtrsim 1$ and show no clear bowing effect.

B. RCP spectra at zero temperature

The RCP spectra for $2\leqslant\nu\leqslant 3$ calculated for $d/l=0$, 0.5, and 5 also show interesting features as shown in Fig. 8. Those for $d/l=0$ shown in Fig. 8(a) consist of a single δ

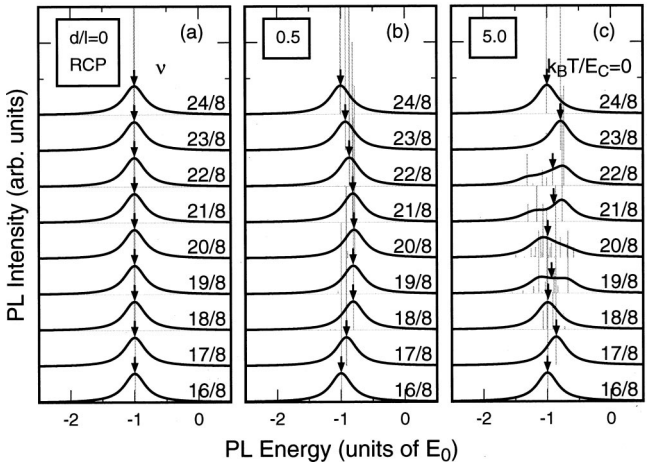

FIG. 8. RCP spectra at $T=0$ calculated at (a) $d/l=0$, (b) 0.5, and (c) 5 in the case $2\leqslant\nu\leqslant3$.

function located at $E=E_-^0-E_0$ independent of the filling factors, because inter-Landau-level *e-e* scattering is forbidden and a kind of the hidden symmetry still survives at $d=0$, as mentioned already in Sec. I. Screening effects in the initial and final states are exactly canceled out in the PL energy.

When the *e-h* layer distance is increased, this symmetry is destroyed, because the *e-h* interaction becomes small and the cancellation is incomplete. In fact, the PL energy is shifted showing an upward convex curve for $d/l\sim0.5$, as shown in Fig. 8(b). At large *e-h* layer distance $d\gg l$, spectra are highly broadened and show no clear bowing effect, as shown in Fig. 8(c). This is presumably because a strong *e-e* interaction suppresses the screening effect as has been discussed in the previous section.

The PL energy is blueshifted discontinuously at $\nu=2^+$ for $d\neq0$. In this case, both initial and final states consist of a single exciton. Because the binding energy of the exciton in the initial state is smaller than that in the final state, the PL energy is shifted to the high-energy side.

The RCP spectra for $3\leqslant\nu\leqslant4$ calculated at $d/l=0$, 0.5, and 5 are shown in Fig. 9. As in the case of the LCP spectra,

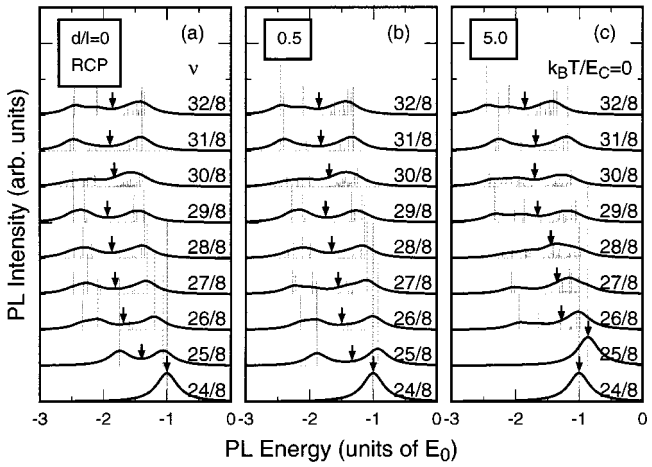

FIG. 9. RCP spectra at $T=0$ calculated at (a) $d/l=0$, (b) 0.5, and (c) 5 in the case $3\leqslant\nu\leqslant4$.

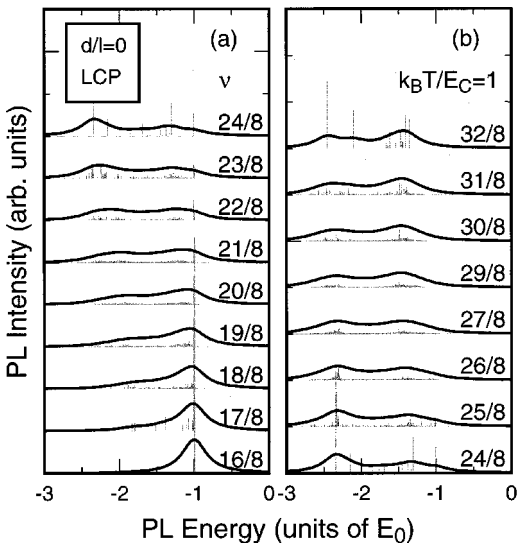

FIG. 10. LCP spectra at high temperature $T=E_C$ calculated at $d/l=0$ in the cases (a) $2\leqslant\nu\leqslant3$ and (b) $3\leqslant\nu\leqslant4$.

they consist of a large number of δ functions, but show a two-peak structure if a sufficiently large broadening is introduced. When the *e-h* layer distance is small ($d/l\leqslant1$), two peaks have comparable intensities and are both shifted to the lower-energy side, showing a downward convex curve in the ν dependence. As the *e-h* layer distance d/l increases, such a bowing effect in the energy shifts is suppressed and the broadening of the spectra is enhanced.

As will be discussed in Sec. V, the RCP spectra at $\nu=3^+$ are similar to LCP at $\nu=2^+$ in their structure. In fact, they show a two-peak structure when $d/l=0$ and 0.5, but only a single peak suddenly shifted to the low-energy side at $d/l=5$.

C. Spectra at finite temperature

Next, we consider the PL spectra at a high temperature $k_BT/E_C=1$ in the large Zeeman limit. The LCP spectra cal-

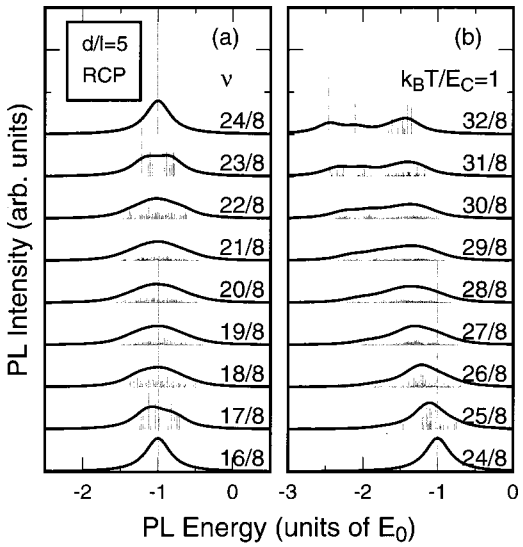

FIG. 11. RCP spectra at high temperature $T=E_C$ calculated at $d/l=5$ in the cases (a) $2\leqslant\nu\leqslant3$ and (b) $3\leqslant\nu\leqslant4$.

culated at $d/l=0$ for $2\leqslant\nu\leqslant3$ and $3\leqslant\nu\leqslant4$ are shown in Figs. 10(a) and 10(b), respectively. Again, they consist of a tremendously large number of δ functions, but it seems that the broadened spectra show basically a double-peak structure. In the whole range of $2<\nu\leqslant4$, the spectra show two peaks and both low- and high-energy peaks show an almost linear ν energy shift.

The RCP spectra calculated for $d/l=5$ at a high temperature $k_BT/E_C=1$ are shown in Fig. 11. Because of the remaining hidden symmetry, the RCP spectra at $d/l=0$ for $2\leqslant\nu\leqslant3$ show no temperature dependence and are still given by Fig. 8(a). When d is increased, the peak is highly broadened, but its average position is not so changed as is shown in Fig. 11(a). In the case $3\leqslant\nu\leqslant4$, the single peak at $\nu=3$ splits into two peaks as the filling factor ν is increased.

In short, the basic structure of spectra (the number of peaks) is almost independent of temperature. However, the bowing effects in PL energy shifts, which are caused by the screening effect at low temperature, are suppressed at a high temperature.

V. PL SPECTRA AROUND FILLING 2

As has been shown in Sec. IV, the LCP spectra obtained by the finite-size calculation at $T=0$ show a sudden peak splitting at $\nu=2^+$, when the *e-h* layer distance is not so large ($d\leqslant l$). To treat this sudden splitting more rigorously, we analytically calculate the PL spectra in the thermodynamic limit ($N_\phi\to\infty$) at $\nu=2$ and 2^+. This analysis also gives us physical insight into the origin of peak splitting shown in LCP spectra at $\nu>2$.

First, we consider the PL spectra just at $\nu=2$. The initial states of the LCP and RCP photoemission have N_ϕ-fold degeneracy and are written as

$$|X\rangle_{i,-}=h^\dagger_{0X-}|2\rangle,$$

$$|X\rangle_{i,+}=h^\dagger_{0X+}|2\rangle, \tag{5.1}$$

respectively, where $|2\rangle$ denotes filled lowest Landau level. They have the energies

$$E_{i,-}=E(2)+\epsilon^h_{0-},$$

$$E_{i,+}=E(2)+\epsilon^h_{0+}, \tag{5.2}$$

where $E(2)$ denotes the energy of the $\nu=2$ QH state. The final states are also given by

$$|X\rangle_{f,-}=\mathcal{L}_-|X\rangle_{i,-}=e_{0X+}|2\rangle,$$

$$|X\rangle_{f,+}=\mathcal{L}_+|X\rangle_{i,+}=e_{0X-}|2\rangle, \tag{5.3}$$

whose energies are given by

$$E_{f,-}=E(2)-\epsilon^e_{0+}+E_0,$$

$$E_{f,+}=E(2)-\epsilon^e_{0-}+E_0. \tag{5.4}$$

Thus PL spectra are calculated as

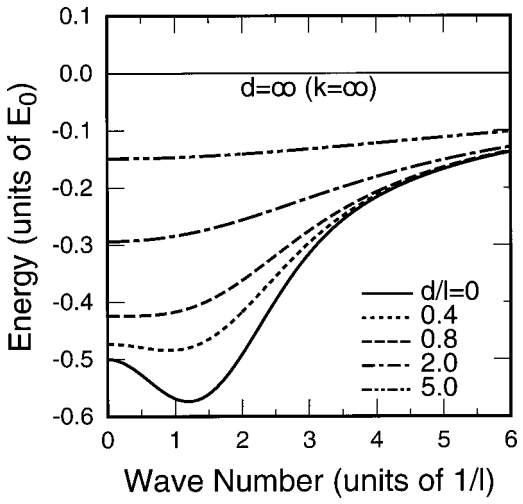

FIG. 12. Effective interaction between an electron in the first excited Landau level and a valence hole in the lowest Landau level. The horizontal axis *kl* denotes the *e-h* distance of guiding center coordinates projected onto the *xy* plane in units of *l*. The results of $d/l=0$, 0.4, 0.8, 2, and 5 are shown with solid, dotted, dashed, dash-single-dotted, and dash-double-dotted lines, respectively. $E=0$ denotes the pair energy of an electron in the first excited Landau level and a hole in the lowest Landau level separated infinitely in distance (i.e., $d\to\infty$ or $k\to\infty$).

$$\tilde{P}_\alpha(E)=\delta(E-E^0_\alpha+E_0), \tag{5.5}$$

independently of the *e-h* layer distance *d*.

Second, we consider the spectra at $\nu=2^+$ and $T=0$. The ground initial states of the LCP and RCP photoemission are the exciton states with wave vector $\mathbf{k}$ written as

$$|\mathbf{k}\rangle_{i,-}=\frac{1}{\sqrt{N_\phi}}\sum_{XX'}B^{XX'}_{\mathbf{k}}e^\dagger_{1X+}h^\dagger_{0X'-}|2\rangle,$$

$$|\mathbf{k}\rangle_{i,+}=\frac{1}{\sqrt{N_\phi}}\sum_{XX'}B^{XX'}_{\mathbf{k}}e^\dagger_{1X+}h^\dagger_{0X'+}|2\rangle. \tag{5.6}$$

Their energies are given by

$$E_{i,-}(k)=E(2)+\epsilon^e_{1+}-E_1+\epsilon^h_{0-}+E^1_X(k,d),$$

$$E_{i,+}(k)=E(2)+\epsilon^e_{1+}-E_1+\epsilon^h_{0+}+E^1_X(k,d), \tag{5.7}$$

respectively, where the interaction between an electron in the first excited Landau level and a valence hole in the lowest level is calculated as

$$E^1_X(k,d)=\frac{1}{A}\sum_{\mathbf{q}\neq0}v^{eh}_qA^{11}_{-\mathbf{q}}A^{00}_{\mathbf{q}}\exp[-i(\mathbf{k}\times\mathbf{q})_zl^2]$$

$$\to\frac{1}{(2\pi)^2}\int_0^\infty q\,dq\,A^{11}_qA^{00}_qv^{eh}_qJ_0(qkl^2)\quad(N_\phi\to\infty), \tag{5.8}$$

with the lowest-order Bessel function $J_0(x)$. The energy dispersion $E^1_X(k,d)$ is calculated for various value of d and

shown in Fig. 12. When the *e-h* layer distance d is smaller than a critical value d_c, they show a minimum at $k=k_R \neq 0$ (a roton minimum). If the *e-h* layer distance d is larger than d_c, they show a minimum at $k=0$. The critical distance is calculated as $d_c/l=0.7773...$.

To obtain the final state of the LCP photoemission, we introduce the bright (optically allowed) and dark (optically forbidden) exciton states as

$$|\mathbf{k}\rangle_b=\mathcal{L}_-|\mathbf{k}\rangle_{i-}=\frac{1}{\sqrt{N_\phi}}\sum_{XX'} B_{\mathbf{k}}^{XX'} e_{1X+}^\dagger e_{0X'+}|2\rangle,$$

$$|\mathbf{k}\rangle_d=-\frac{1}{\sqrt{N_\phi}}\sum_{XX'} B_{\mathbf{k}}^{XX'} e_{1X-}^\dagger e_{0X'-}|2\rangle. \tag{5.9}$$

They are coupled with and only with each other through opposite-spin scattering. On the other hand, same-spin scattering gives their energy shifts. The effective Hamiltonian for the finals states is reduced to a 2×2 matrix whose elements are calculated as

$$\begin{aligned}{}_b\langle\mathbf{k}|\mathcal{H}|\mathbf{k}\rangle_b={}_d\langle\mathbf{k}|\mathcal{H}|\mathbf{k}\rangle_d&=E(2)+\epsilon_{1+}^e-E_1-\epsilon_{0+}^e+E_0\\&\quad+E_X^1(k,0)+\Delta(k),\\{}_b\langle\mathbf{k}|\mathcal{H}|\mathbf{k}\rangle_d={}_d\langle\mathbf{k}|\mathcal{H}|\mathbf{k}\rangle_b&=-\Delta(k),\end{aligned} \tag{5.10}$$

where $\Delta(k)$ denotes the inter-Landau-level scattering:

$$\Delta(k)=\frac{1}{2\pi l^2}|A_{\mathbf{k}}^{10}|^2 v_k^{ee}. \tag{5.11}$$

The coupling constant $\Delta(k)$ vanishes when and only when $k=0$. In this case, the bright final state $|\mathbf{k}\rangle_b$ becomes an energy eigenstate and the spectrum is given by a single δ function. Otherwise, the bright and dark states are coupled to each other through opposite-spin scattering, and mode repulsion leads to a peak splitting in the PL spectrum.

Diagonalizing this effective Hamiltonian matrix, we obtain spin-triplet and -singlet states

$$|\mathbf{k};t\rangle_{f-}=\frac{1}{\sqrt{2}}(|\mathbf{k}\rangle_b+|\mathbf{k}\rangle_d),$$

$$|\mathbf{k};s\rangle_{f-}=\frac{1}{\sqrt{2}}(|\mathbf{k}\rangle_b-|\mathbf{k}\rangle_d), \tag{5.12}$$

with energies

$$\begin{aligned}E_{f-}(k;t)&=E(2)+\epsilon_{1+}^e-E_1-\epsilon_{0+}^e+E_0+E_X^1(k,0),\\E_{f-}(k;s)&=E(2)+\epsilon_{1+}^e-E_1-\epsilon_{0+}^e+E_0+E_X^1(k,0)+2\Delta(k)\end{aligned} \tag{5.13}$$

These results are nothing but the energy dispersions of the cyclotron mode obtained in Refs. 64–69. It is interesting to note that the inter-Landau-level scattering can be regarded as the exchange interaction between the conduction electron in the first excited Landau level and the ''conduction hole'' in the lowest Landau level at $\nu=2^+$. Only the singlet exciton is influenced by the *e-h* exchange interaction.[70]

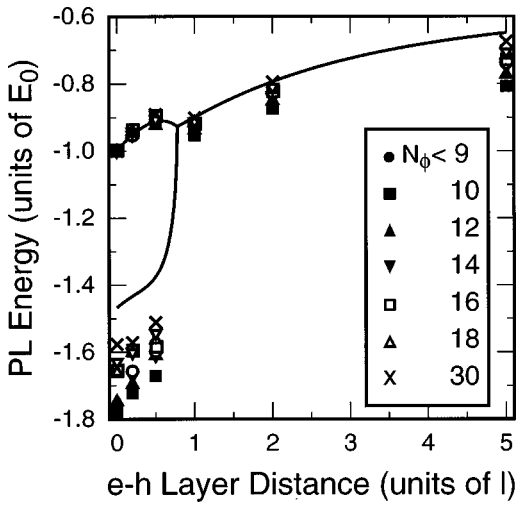

FIG. 13. Peak splitting at $\nu=2^+$ as a function of the *e-h* layer distance d/l. The analytical result in the thermodynamic limit ($N_\phi\to\infty$) is shown with solid lines. The numerical results for $N_\phi<9$, $N_\phi=10$, 12, 14, 16, 18, and 30 are shown with solid circles, solid squares, solid triangles, inverted triangles, open squares, open triangles, and crosses, respectively.

The absence of inter-Landau-level *e-e* scattering at $k=0$ is related to Kohn's theorem, which states

$$E_{f-}(k;t)=E_{f-}(k;s)=E(2)+\epsilon_{1+}^e-\epsilon_{0+}^e \tag{5.14}$$

at $k=0$. [Note the identity $E_0-E_1+E_X^1(0,0)=0$.] If the initial state is always realized at $k=0$, Kohn's theorem implies that the LCP spectrum consists of a single peak at $\nu=2^+$ and is suddenly blueshifted when the filling factor is increased across 2.[54] In fact, we obtain

$$\tilde{P}_-(E)=\delta[E-E_-^0+E_0-E_X^1(0,d)+E_X^1(0,0)], \tag{5.15}$$

which leads to a sudden blueshift due to the inequality $E_X^1(0,0)<E_X^1(0,d)<0$. Note that a similar discontinuous blueshift is also observed around at $\nu=1$.[56–59]

However, when the *e-h* layer distance d is smaller than d_c and the initial-state energy $E_{i-}(k)$ shows a roton minimum at $k=k_R\neq 0$, the spectrum suddenly splits into two lines with an increase of ν from 2 to 2^+. The spectrum at $\nu=2^+$ is given by

$$\begin{aligned}\tilde{P}_-(E)&=\tfrac{1}{2}\,\delta[E-E_-^0+E_0-E_X^1(k_R,d)+E_X^1(k_R,0)]\\&\quad+\tfrac{1}{2}\,\delta[E-E_-^0+E_0-E_X^1(k_R,d)\\&\quad+E_X^1(k_R,0)+2\Delta(k_R)].\end{aligned} \tag{5.16}$$

The discontinuous peak splitting or blueshifts around at $\nu=2$ is plotted as a function of the *e-h* layer distance d/l in

Fig. 13 together with corresponding numerical results obtained in finite-size systems. With the increase of d, two peaks of the LCP spectra increase in energy, come closer together, and finally merge into a single peak at $d=d_c$. The numerical results for finite-size systems are in good agreement with the analytical results.

For the RCP photoemission, the final state is the bright exciton state $|\mathbf{k}\rangle_{f+}=\mathcal{L}_+|\mathbf{k}\rangle_{i+}$ with energy

$$E_{f+}(k)=E(2)+\epsilon^e_{1+}-E_1-\epsilon^e_{0-}+E_0+E^1_X(k,0). \tag{5.17}$$

The spectrum is therefore calculated as

$$\tilde{P}_+(E)=\begin{cases}\delta[E-E^0_++E_0-E^1_X(k_R,d)+E^1_X(k_R,0)] & (d\leqslant d_c),\\ \delta[E-E^0_++E_0-E^1_X(0,d)+E^1_X(0,0)] & (d>d_c),\end{cases} \tag{5.18}$$

which does not show an anomaly at $d=0$, but a discontinuous blueshift for $d\neq 0$ when the filling factor is increased across $\nu=2$. The numerical results are consistent with this analytical prediction again.

The RCP spectra at $\nu=3^+$ exhibit a behavior similar to that of LCP spectra at $\nu=2^+$. The initial state for the RCP emission at $\nu=3^+$ is written as

$$|\mathbf{k}\rangle_{i,+}=\frac{1}{\sqrt{N_\phi}}\sum_{XX'}B^{XX'}_{\mathbf{k}}e^\dagger_{1X-}h^\dagger_{0X'+}|3\rangle,$$

and its energy is given by

$$E_{i,+}(k)=E(3)+\epsilon^e_{1-}-E_1+\epsilon^h_{0+}+E^1_X(k,d),$$

where $|3\rangle$ and $E(3)$ denote the $\nu=3$ integer QH state and its energy, respectively. The ground state is realized at $k\neq 0$ when $d<d_c$ and at $k=0$ when $d\geqslant d_c$. Similar to the case of LCP spectra at $\nu=2^+$, we can introduce the bright and dark states defined by

$$|\mathbf{k}\rangle_b=\mathcal{L}_+|\mathbf{k}\rangle_{i+}=\frac{1}{\sqrt{N_\phi}}\sum_{XX'}B^{XX'}_{\mathbf{k}}e^\dagger_{1X-}e_{0X'-}|3\rangle,$$

$$|\mathbf{k}\rangle_d=-\frac{1}{\sqrt{N_\phi}}\sum_{XX'}B^{XX'}_{\mathbf{k}}e^\dagger_{2X+}e_{1X'+}|3\rangle, \tag{5.19}$$

which are coupled with and only with each other through opposite-spin scattering. The coupling constant between them is given by

$${}_b\langle\mathbf{k}|\mathcal{H}|\mathbf{k}\rangle_d=-\frac{1}{2\pi l^2}A^{10}_{\mathbf{k}}A^{12}_{-\mathbf{k}}v^{ee}_k, \tag{5.20}$$

which vanishes when and only when $k=0$. Therefore, the RCP spectra at $\nu=3^+$ have two peaks at $d<d_c$ caused by the mode repulsion and a single peak at $d\geqslant d_c$ because of the vanishing of the mode coupling.

VI. DISCUSSION

A. Origin of double-peak structure

The numerically obtained LCP spectra in the large Zeeman limit show a double-peak structure independent of the filling factor $2<\nu\leqslant 4$, *e-h* layer distance d, and temperature k_BT. Our calculation shows that the opposite-spin scattering is especially important in such a peak splitting. In fact, the spectra in a spinless system, which gives spectra equivalent for those calculated without opposite-spin scattering, show only a single peak.

The origin of the double-peak structure is mode repulsion between the bright final state $\mathcal{L}_-|i\rangle$ and dark final states caused by strong opposite-spin scattering. The analytical calculation at $\nu=2^+$ clearly supports this mechanism. When the filling factor increases, dark states increase in their number and form an energy continuum. The mode repulsion remains essentially same as long as the hybridization between the bright and dark states is strong enough. This picture of peak splitting is essentially equivalent to that pointed out previously at $\nu=3$.[54]

There are two different types of same-spin scattering processes. In processes of the first type, an electron is relaxed from the first excited to the lowest Landau level and another is excited from the lowest to first excited. These processes contribute mainly to the PL energy shifts as has been discussed in Sec. III. In the second type processes, an electron is relaxed from the first excited to the lowest Landau level and another is excited from the first to second excited. These processes play roles similar to opposite-spin scattering and cause mode repulsion between the bright and dark states. However, the coupling is not strong enough to cause peak splitting and leads to spectral broadening only as seen in spectra in the spinless system. This is presumably because same-spin scattering is much weaker than opposite-spin scattering due to Pauli's exclusion principle.

B. Spin-flipping effects on PL spectra

In the numerical calculations shown above, we have focused on PL in the large Zeeman limit. However, experiments are often performed in systems with a small g factor such as GaAs/AlGaAs heterostructures. The numerical calculation shows that the ground state is maximally spin polarized even in the vanishing Zeeman limit when $\nu>2$. Moreover, PL spectra calculated numerically for the fixed electron spin polarization show a weak temperature dependence in

their basic features. Therefore, it can be expected that the main role of temperature increase is spin flipping in such systems.

To investigate this effect, we consider the LCP spectra $P_{S_z}(E)$ at absolute zero temperature fixing the z component of total electron spin S_z of the initial state. When we choose a new spin axis in which all electrons in the first excited Landau level have up spin, the conduction hole created by the recombination becomes a linear combination of $-\hbar/2$ and $+\hbar/2$ spin states, each of which contributes independently to the PL spectra. The intensity of these contributions is proportional to S_z/S and $(1-S_z/S)$, respectively, where S denotes the total electron spin of the initial state. Therefore, we obtain

$$P_{S_z}(E)=\frac{S_z}{S}P_{S_z=S}(E)+\frac{S-S_z}{S}P_{S_z=-S}(E). \qquad (6.1)$$

The LCP spectra at $S_z=S$ are already calculated in the large Zeeman limit and show double peaks located at $E-E_-^0\sim -E_0$ and $-2E_0$. On the other hand, the LCP spectra at $S_z=-S$ are equivalent to the RCP spectra and exhibit a single peak at $E-E_-^0=-E_0$. Thus the spin-flipping enhances the high-energy peak located at $E-E_-^0\sim -E_0$.

This result qualitatively explains the recent experimental results.[22–25] The experiments always show a double-peak structure when $\nu\gtrsim 2$. In Refs. 22 and 24, the high-energy peak is labeled as LL_0 and the low-energy peak is denoted by SU_0 or OA_0. They show that the low-energy peak is enhanced with a decrease of the temperature.

VII. SUMMARY

We study the PL spectra in quantum Hall systems of filling factor $\nu\geqslant 2$ using a numerical diagonalization method, considering the spin degree of freedom for the electrons and valence hole. The averaged energy of luminescence shows a ν dependence explained by screening effects. The calculated spectra of the LCP photoemission usually show a double-peak structure in the region $2<\nu\leqslant 4$. The RCP spectra show a single peak when $2\leqslant\nu\leqslant 3$ and a double-peak structure when $3\leqslant\nu\leqslant 4$. The origin of the double-peak structure is a strong hybridization between the bright and dark final states through opposite-spin scattering. The results explain the recent experiments qualitatively.

ACKNOWLEDGMENTS

This work is supported in part by Grant-in-Aid for COE Research from the Ministry of Education, Science, Sports, and Culture (12CE2004 ''Control of Electrons by Quantum Dot Structures and Its Application to Advanced Electronics''). Some numerical calculations were performed on HITACHI H9000V L2000 in the Supercomputer Center, Institute for Solid State Physics, University of Tokyo. K.A. would like to thank the JSPS for Young Scientists for financial support.

[1] M. C. Smith, A. Petrou, C. H. Perry, J. M. Worlock, and R. L. Aggarwal, in *Proceedings of the 17th International Conference on the Physics Semiconductors, San Francisco, 1984*, edited by J. D. Chadi and W. A. Harrison (Springer, New York, 1984), p. 547.

[2] D. Heiman, B. B. Goldberg, A. Pinczuk, C. W. Tu, A. C. Gossard, and J. H. English, Phys. Rev. Lett. **61**, 605 (1988).

[3] B. B. Goldberg, D. Heiman, A. Pinczuk, L. Pfeiffer, and K. West, Phys. Rev. Lett. **65**, 641 (1990).

[4] B. B. Goldberg, D. Heiman, M. Dahl, A. Pinczuk, L. Pfeiffer, and K. West, Phys. Rev. B **44**, 4006 (1991).

[5] B. B. Goldberg, D. Heiman, A. Pinczuk, L. Pfeiffer, and K. West, Surf. Sci. **263**, 9 (1992).

[6] B. B. Goldberg, D. Heiman, A. Pinczuk, L. Pfeiffer, and K. West, in *High Magnetic Fields in Semiconductor Physics III*, edited by G. Landwehr (Springer-Verlag, Berlin, 1992), p. 243.

[7] D. Heiman, A. Pinczuk, H. Okamura, M. Dahl, B. S. Dennis, L. N. Pfeiffer, and K. W. West, Physica B **201**, 315 (1994).

[8] S. Takeyama, H. Kunimatsu, K. Uchida, N. Miura, G. Karczewski, J. Jaroszynski, T. Wojtowicz, and J. Kossult, Physica B **246–247**, 200 (1998).

[9] H. Kunimatsu, S. Takeyama, K. Uchida, N. Miura, G. Karczewski, T. Wojtowicz, and J. Kossult, Physica B **249–251**, 951 (1998).

[10] F. Plentz, D. Heiman, L. N. Pfeiffer, and K. W. West, Phys. Rev. B **57**, 1370 (1998).

[11] J. L. Osborne, A. J. Shields, M. Y. Simmons, N. R. Cooper, D. A. Ritchie, and M. Pepper, Phys. Rev. B **58**, 4227 (1998).

[12] A. J. Turberfield, S. R. Haynes, P. A. Wright, R. A. Ford, R. G. Clark, J. F. Ryan, J. J. Harris, and C. T. Foxon, Phys. Rev. Lett. **65**, 637 (1990).

[13] A. J. Turberfield, R. A. Ford, I. N. Harris, J. F. Ryan, C. T. Foxon, and J. J. Harris, Phys. Rev. B **47**, 4794 (1993).

[14] H. D. M. Davies, J. C. Harris, R. L. Brockbank, J. F. Ryan, A. J. Turberfield, M. Simmons, and D. A. Ritchie, Physica B **299–251**, 544 (1998).

[15] E. M. Goldys, S. A. Brown, R. B. Dunford, A. G. Davies, R. Newbury, R. G. Clark, P. E. Simmonds, J. J. Harris, and C. T. Foxon, Phys. Rev. B **46**, 7957 (1992).

[16] R. G. Clark, R. A. Ford, S. R. Haynes, J. F. Ryan, A. J. Turberfield, P. A. Wright, C. T. Foxon, and J. J. Harris, in *High Magnetic Fields in Semiconductor Physics III*, edited by G. Landwehr (Springer-Verlag, Berlin, 1992), p. 231.

[17] R. G. Clark, A. G. Davies, S. A. Brown, R. B. Dunford, P. E. Simmonds, A. C. Lindsay, R. Newbury, R. P. Starrett, A. Skougarevsky, E. E. Mitchell, R. P. Taylor, C. J. Mellor, B. L. Gallagher, C. T. Foxon, and J. J. Harris, Physica B **201**, 301 (1994).

[18] R. J. Nicholas, D. Kinder, A. N. Priest, C. C. Chang, H. H. Chang, J. J. Harris, and C. T. Foxon, Physica B **249–251**, 562 (1998).

[19] H. Buhmann, W. Joss, K. von Klitzing, I. V. Kukushkin, G. Martinez, A. S. Plaut, K. Ploog, and V. B. Timofeev, Phys. Rev. Lett. **65**, 1056 (1990).

[20] I. V. Kukushkin, H. Buhmann, W. Joss, K. von Klitzing, G. Mar-

tinez, S. Plaut, K. Ploog, and V. B. Timofeev, in *High Magnetic Fields in Semiconductor Physics III*, edited by G. Landwehr (Springer-Verlag, Berlin, 1992), p. 217.
[21] I. V. Kukushkin and V. B. Timofeev, Adv. Phys. **45**, 147 (1996).
[22] G. Finkelstein, H. Shtrikman, and I. Bar-Joseph, Phys. Rev. B **56**, 10 326 (1997).
[23] L. Gravier, M. Potemski, P. Hawrylak, and B. Etienne, Phys. Rev. Lett. **80**, 3344 (1998).
[24] M. J. Manfra, B. B. Goldberg, L. Pfeiffer, and K. West, Phys. Rev. B **57**, 9467 (1998).
[25] S. Takeyama, G. Karczewski, J. Jaroszynski, T. Wojtowicz, J. Kossult, H. Kunimatsu, K. Uchida, and N. Miura, Phys. Rev. B **59**, 7327 (1999).
[26] I. V. Lerner and Yu. E. Lozovik, Zh. Eksp. Theor. Fiz. **80**, 1488 (1981) [Sov. Phys. JETP **53**, 763 (1981)].
[27] B. Dzyubenko and Yu. E. Lozovik, Fiz. Tverd. Tela (Leningrad) **25**, 1519 (1983) [Sov. Phys. Solid State **25**, 874 (1983)].
[28] A. H. MacDonald and E. H. Rezayi, Phys. Rev. B **42**, 3224 (1990).
[29] A. H. MacDonald, E. H. Rezayi, and D. Keller, Phys. Rev. B **68**, 1939 (1992).
[30] S. Katayama and T. Ando, Solid State Commun. **70**, 97 (1989).
[31] T. Uenoyama and L. J. Sham, Phys. Rev. B **39**, 11044 (1989).
[32] T. Tsuchiya, S. Katayama, and T. Ando, Jpn. J. Appl. Phys., Suppl. **34**, 240 (1995).
[33] T. Tsuchiya, S. Katayama, and T. Ando, Jpn. J. Appl. Phys., Suppl. **34**, 4544 (1995).
[34] T. Tsuchiya, S. Katayama, and T. Ando, Surf. Sci. **361–362**, 376 (1996).
[35] É. I. Rashba and M. E. Portnoi, Phys. Rev. Lett. **70**, 3315 (1993).
[36] T. V. Tatarinova, É. I. Rashba, and A. L. Efros, Phys. Rev. B **50**, 17 349 (1994).
[37] V. M. Apal'kov and É. I. Rashba, Pis'ma Zh. Eksp. Theor. Fiz. **53**, 46 (1991) [JETP Lett. **53**, 442 (1991)].
[38] V. M. Apal'kov and É. I. Rashba, Pis'ma Zh. Eksp. Theor. Fiz. **53**, 46 (1991) [JETP Lett. **53**, 49 (1991)].
[39] V. M. Apal'kov and É. I. Rashba, Pis'ma Zh. Eksp. Theor. Fiz. **54**, 160 (1991) [JETP Lett. **54**, 155 (1991)].
[40] V. M. Apal'kov and É. I. Rashba, Pis'ma Zh. Eksp. Theor. Fiz. **55**, 38 (1992) [JETP Lett. **55**, 37 (1992)].
[41] V. M. Apal'kov and É. I. Rashba, Phys. Rev. B **46**, 1628 (1992).
[42] V. M. Apal'kov and É. I. Rashba, Phys. Rev. B **48**, 18 312 (1993).
[43] V. M. Apal'kov, F. G. Pikus, and É. I. Rashba, Phys. Rev. B **52**, 6111 (1995).
[44] X. M. Chen and J. J. Quinn, Phys. Rev. Lett. **70**, 2130 (1993).
[45] X. M. Chen and J. J. Quinn, Phys. Rev. B **50**, 2354 (1994).
[46] X. M. Chen and J. J. Quinn, Solid State Commun. **92**, 865 (1994).
[47] J. Zang and J. Birman, Phys. Rev. B **51**, 5574 (1995).
[48] A. Wójs, J. J. Quinn, and P. Hawrylak, Phys. Rev. B **62**, 4630 (2000).
[49] A. Wójs and J. J. Quinn, Phys. Rev. B **63**, 045303 (2000).
[50] A. Wójs and J. J. Quinn, Phys. Rev. B **63**, 045304 (2000).
[51] T. Chakraborty and P. Pietiläinen, Phys. Rev. B **44**, 13 078 (1991).
[52] K. Asano and T. Ando, Physica B **249–251**, 549 (1998).
[53] K. Asano and T. Ando, Physica B **256–258**, 319 (1998).
[54] P. Hawrylak and M. Potemski, Phys. Rev. B **56**, 12 386 (1997).
[55] K. Asano and T. Ando, Physica E **7**, 604 (2000).
[56] B. A. Muzykantkii, Zh. Eksp. Theor. Fiz. **101**, 1084 (1992) [Sov. Phys. JETP **74**, 897 (1992)].
[57] N. R. Cooper and D. B. Chkolovskii, Phys. Rev. B **55**, 2436 (1997).
[58] T. Portengen, J. R. Chapman, V. N. Nicopoulos, and N. F. Johanson, Phys. Rev. B **55**, 7367 (1997).
[59] T. Portengen, J. R. Chapman, V. N. Nicopoulos, and N. F. Johanson, Phys. Rev. B **56**, 10 052 (1997).
[60] D. Yoshioka, Phys. Rev. B **29**, 6833 (1984).
[61] D. Yoshioka, J. Phys. Soc. Jpn. **55**, 885 (1986).
[62] D. Yoshioka, J. Phys. Soc. Jpn. **55**, 3960 (1986).
[63] F. D. M. Haldane, Phys. Rev. Lett. **55**, 2095 (1985).
[64] I. V. Lerner and Yu. E. Lozovik, Zh. Eksp. Theor. Fiz. **78**, 1167 (1978) [Sov. Phys. JETP **51**, 588 (1980)].
[65] Yu. A. Bychkov, S. V. Iordanskii, and G. M. Eliashberg, Zh. Eksp. Theor. Fiz. **33**, 152 (1981) [JETP Lett. **33**, 143 (1981)].
[66] C. Kallin and B. I. Halperin, Phys. Rev. B **30**, 5655 (1981).
[67] C. Kallin, in *Interfaces, Quantum Wells and Superlattices*, edited by C. R. Leavens and R. Taylor (Plenum, New York, 1988), p. 163.
[68] A. H. MacDonald, J. Phys. C **18**, 1003 (1985).
[69] Yu. E. Lozovik and A. M. Ruvinskii, Zh. Eksp. Theor. Fiz. **112**, 1791 (1997) [Sov. Phys. JETP **85**, 979 (1997)].
[70] S. Nakajima, Y. Toyozawa, and R. Abe, *The Physics of Elementary Excitations* (Springer-Verlag, Berlin, 1980), p. 82.